European Journal of Medicinal Chemistry 63 (2013) 33–45

Contents lists available at SciVerse ScienceDirect

European Journal of Medicinal Chemistry

journal homepage: http://www.elsevier.com/locate/ejmech

Original article

Nonclassical antifolates, part 3: Synthesis, biological evaluation and molecular modeling study of some new 2-heteroarylthio-quinazolin-4-ones☆

Fatmah A.M. Al-Omary [a], Ghada S. Hassan [a,b], Shahenda M. El-Messery [c], Mahmoud N. Nagi [d], El-Sayed E. Habib [e], Hussein I. El-Subbagh [f,*]

[a] Department of Pharmaceutical Chemistry, College of Pharmacy, King Saud University, P.O. Box 2457, Riyadh 11451, Saudi Arabia
[b] Department of Medicinal Chemistry, Faculty of Pharmacy, Mansoura University, 35516 Mansoura, Egypt
[c] Department of Pharmaceutical Organic Chemistry, Faculty of Pharmacy, Mansoura University, 35516 Mansoura, Egypt
[d] Department of Pharmacology, College of Pharmacy, King Saud University, P.O. Box 2457, Riyadh 11451, Saudi Arabia
[e] Department of Pharmaceutics and Pharmaceutical Technology (Microbiology), College of Pharmacy, Taibah University, Almadinah Almunawwarah 344, Saudi Arabia
[f] Department of Pharmaceutical Chemistry, Faculty of Pharmaceutical Sciences & Pharmaceutical Industries, Future University, 12311 Cairo, Egypt

ARTICLE INFO

Article history:
Received 8 September 2012
Received in revised form
24 December 2012
Accepted 26 December 2012
Available online 13 February 2013

Keywords:
Synthesis
Quinazolin-4-ones
DHFR inhibition
Antimicrobial testing
Antitumor screening
Molecular modeling study

ABSTRACT

A new series of 2-heteroarylthio-6-substituted-quinazolin-4-one analogs was designed, synthesized, and evaluated for their *in vitro* DHFR inhibition, antimicrobial, and antitumor activities. Compounds **21**, **25**, and **39** proved to be active DHFR inhibitors with IC_{50} range of 0.3–0.8 μM. Compounds **25**, **28**, **33**, **35** and **36** showed broad spectrum antimicrobial activity comparable to the known antibiotic gentamicin. Compound **29** showed broad spectrum antitumor activity toward several tumor cell lines with GI values range of 25.8–41.2%. Molecular modeling studies concluded that recognition with key amino acid Arg38 and Lys31 are essential for binding and biological activities. Flexible alignment; electrostatic and hydrophobic mappings revealed that the obtained model could be useful for the development of new DHFR inhibitors.

1. Introduction

Dihydrofolate reductase (DHFR) plays a crucial role in the biosynthesis of nucleic acids. It catalyzes the NADPH reduction of 7,8-dihydrofolate to 5,6,7,8-tetrahydrofolate and intimately couples with thymidylate synthase. Thymidylate synthase is the key enzyme that catalyzes the reductive methylation of deoxyuridine monophosphate (dUMP) to deoxythymidine monophosphate (dTMP) utilizing N^5,N^{10}-methylene-tetrahydrofolate as a cofactor. Hence, the inhibition of DHFR or thymidylate synthase activity leads to cellular deficiency of tetrahydrofolate cofactors, that results in disruption of the biosynthesis of purines and pyrimidines, and finally to cell death [1,2]. Thus, DHFR inhibition has long been identified as an important target for the development of chemotherapeutic agents against bacterial and parasitic infections as well as cancer [3].

DHFR inhibitors are broadly classified as either classical or nonclassical antifolates. The classical antifolates possess p-aminobenzoylglutamate side-chain embedded in the molecule, whereas non-classical inhibitors of DHFR does not possess the glutamate moiety, but rather have a lipophilic side-chain. Literature citations revealed numerous compounds which categorized under the nonclassical DHFR inhibitors such as: trimethoprim (TMP, **1**), trimetrexate (TMQ, **2**) and piritrexim (PTX, **3**), beside others belong to the quinazoline heterocycle [4–12], (Chart 1).

Recently, a new series of 2,6-substituted-quinazolin-4-ones was designed, synthesized, and evaluated for their *in vitro* DHFR inhibition in our laboratories [13,14]. This study allowed the allocation of compounds **4**–**8** as active DHFR inhibitors with IC_{50} values around 0.4 μM (Chart 1). Compounds **6** and **8** characterized by bearing 2-thioallylic hydrophobic π-system. Molecular modeling studies of this class of compounds revealed the importance of the main pharmacophoric groups (the 4-carbonyl fragment, the basic nitrogen atom at N-1, and the hydrophobic π-system regions) as

☆ For parts 1 and 2 see Refs. [13,14].

* Corresponding author. Tel./fax: +20 2 26186111.
E-mail address: subbagh@yahoo.com (H.I. El-Subbagh).

0223-5234/$ – see front matter © 2013 Elsevier Masson SAS. All rights reserved.
http://dx.doi.org/10.1016/j.ejmech.2012.12.061

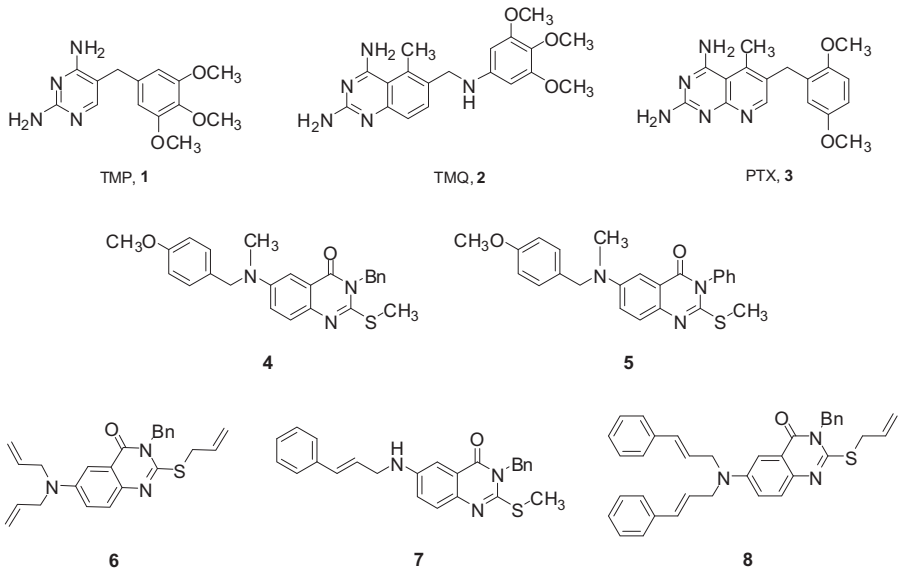

Chart 1. Structures of literature antifolate lead compounds.

well as of their relative spatial distances. The substitution pattern and spatial considerations of the π-systems in regard to the quinazoline nucleus proved to be critical for DHFR inhibition [13,14].

In continuation to our previous efforts [13–27], a new series of 2-arylthio or heteroarylthio-quinazolin-4-one analogs, of the general formula presented in Chart 2 was designed to possess 2-arylthio or heteroarylthio functions as hydrophobic π-system regions replacing the 2-thioalkyl and 2-thioallyl function of **4**–**8**. In addition, 6-chloro, 6-methyl, or 6,7-dimethoxy functions, representing electron donating and electron withdrawing substituents; a phenyl or benzyl group at position 3 were introduced to the quinazolin-4-one nucleus in resemblance to the lead compounds **4**–**8**. Most of the functions designed to be accommodated on the quinazoline ring such as thioether, aryl, heteroaryl groups are known to contribute to DHFR inhibition activity [28,29]. The aim of this study is to locate novel synthetic lead compound(s), and their *in vitro* testing as DHFR inhibitor(s). In addition, these derivatives were tested for their *in vitro* antimicrobial activity against a panel of standard strains of Gram-positive and Gram-negative bacteria. Furthermore, the new compounds were screened for their *in vitro* antitumor activity using the NCI's disease-oriented human cell lines assay [30–33]. Compounds possessing DHFR inhibition activity will be the candidates for treating cancer and bacterial or parasitic infections.

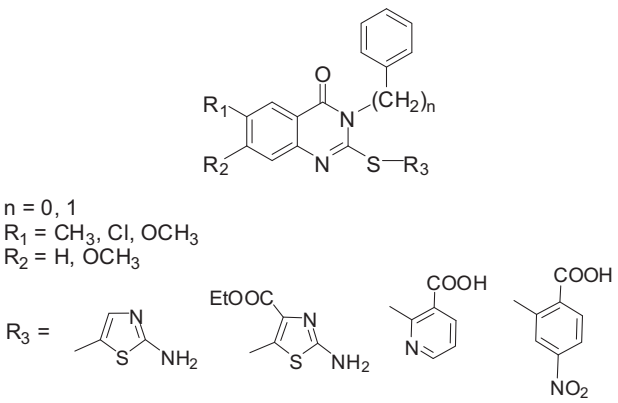

Chart 2. Structures of the designed new DHFR inhibitors.

2. Results and discussion

2.1. Chemistry

The synthetic strategy to obtain the targets of the general formula presented in Chart 2 is depicted in Scheme 1. The starting materials 2-mercapto-6-methyl-3-phenyl (or benzyl)-quinazolin-4(3*H*)-ones (**14**, **15**), 6-chloro-2-mercapto-3-phenyl (or benzyl)-quinazolin-4(3*H*)-ones (**16**, **17**) and 6,7-dimethoxy-2-mercapto-3-phenyl (or benzyl)-quinazolin-4(3*H*)-ones (**18**, **19**) were prepared adopting reported procedures [24–26]. The 2-thioxo-function of the starting materials **14**–**19** was then alkylated using variety of halogenated aryl or heteroaryl derivatives.

Compounds **14**–**19** were reacted with 5-bromothiazole-2-amine (**20**), 2-chloronicotinic acid (**27**), ethyl 2-amino-5-bromothiazole-4-carboxylate (**34**) or 2-chloro-4-nitrobenzoic acid (**41**) and potassium carbonate in dimethylformamide to afford 2-(2-aminothiazol-5-ylthio)-3-phenyl (or benzyl)-6-substituted (or 6,7-dimethoxy)-quinazolin-4(3*H*)-ones (**21**–**26**), 2-(3-benzyl-6-substituted (or 6,7-dimethoxy)-4-oxo-3,4-dihydro quinazoline-2-ylthio)nicotinic acid derivatives (**28**–**33**), ethyl 2-amino-5-(3-phenyl (or benzyl)-6-substituted (or 6,7-dimethoxy)-4-oxo-3,4-dihydroquinazolin-2-ylthio)thiazole-4-carboxylate analogs (**35**–**40**) or 2-(3-phenyl (or benzyl)-6-substituted (or 6,7-dimethoxy)-4-oxo-3,4-dihydroquinazolin-2-ylthio)-4-nitrobenzoic acid derivatives (**42**–**47**), respectively, Scheme 1. Structure elucidation of the synthesized intermediates and final products was attained by the aid of elementary analyses, ^{1}H & ^{13}C NMR spectroscopy, and mass spectrometry.

2.2. Dihydrofolate reductase (DHFR) inhibition

The synthesized compounds (**21**–**47**) were evaluated as inhibitors of bovine liver DHFR using reported procedure [34]. Results were reported as IC_{50} values (Tables 2 and 3). Compounds **21**, **22**, **25**, **35**, **38**, and **39** proved to be the most active DHFR inhibitors with IC_{50} values range of 0.3–1.0 μM, while compounds **23**, **24**, **26**, **36**, **37**, **40**, and **47** were considered of moderate activity with IC_{50} range of

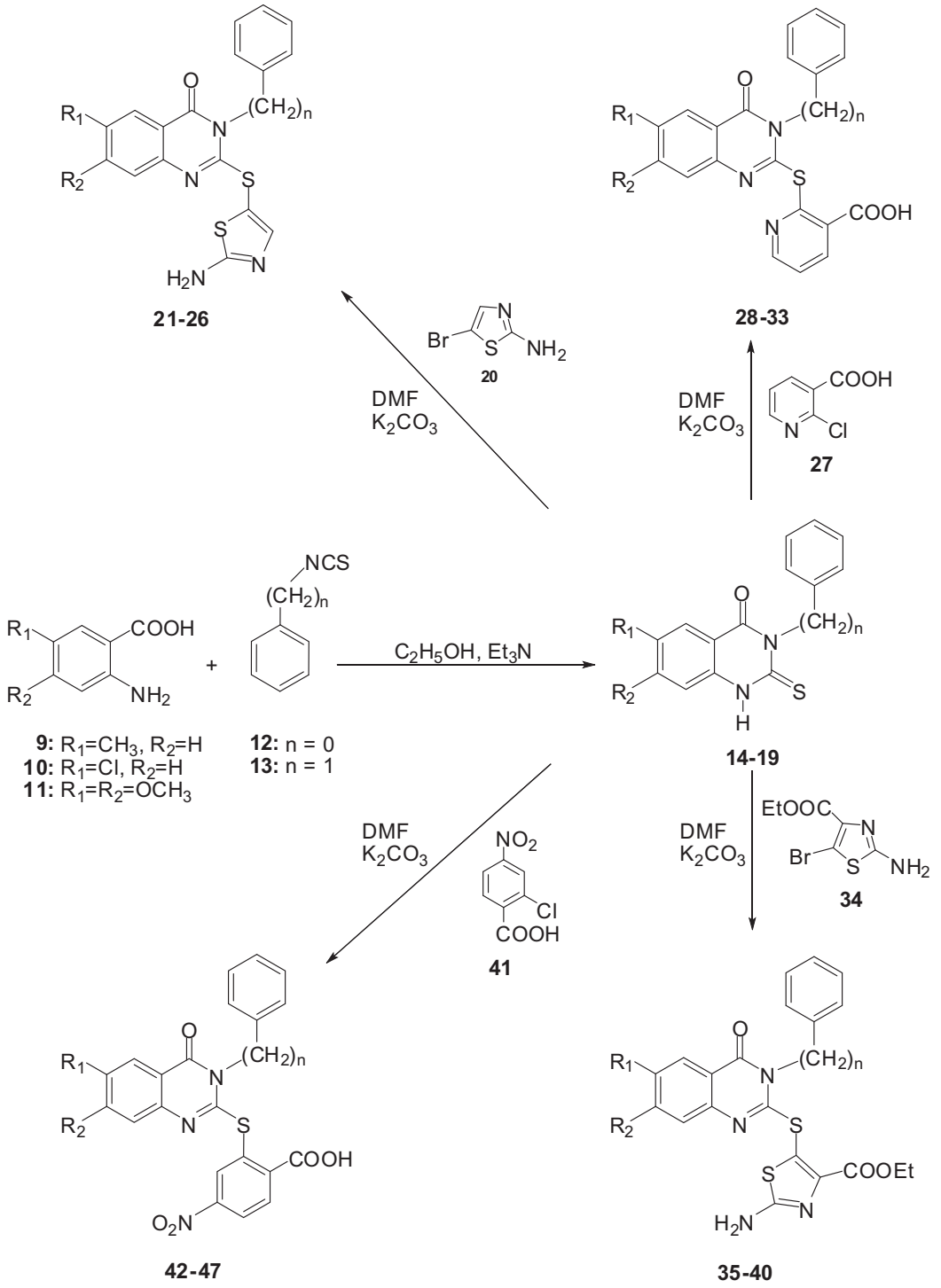

Scheme 1. Synthesis of the target compounds **21**–**47**.

1.0–5.0 μM, the rest of the tested compounds were considered inactive with $IC_{50} > 5$ μM. Methotrexate (IC_{50} 0.08 μM) was used as a positive control.

2.2.1. Structure activity relationship (SAR)

In the present investigation, the type of 2-, 3- or 6-substituent on the studied quinazolines manipulated the DHFR inhibition activity. Four different groups of compounds were synthesized differ in the type of the 2-thioether function attached to the used quinazoline analogs, namely, 2-aminothiazole (**21**–**26**), 2-nicotinic acid (**28**–**33**), ethyl 2-aminothiazole-4-carboxylate (**35**–**40**) or 4-nitrobenzoic acid derivatives (**42**–**47**). The 2-thioether function affects the magnitude of DHFR inhibition. The order of activity is 2-aminothiazole or ethyl 2-aminothiazole-4-carboxylate (IC_{50} 0.3–4.0 μM) > 2-nicotinic acid or 4-nitrobenzoic acid (IC_{50} 7.0–12.0 μM). In the 6-methyl series, the presence of 3-phenyl and 2-aminothiazole-5-thiol produced **21** with IC_{50} 0.8 μM; replacing of the 3-phenyl by 3-benzyl or the introduction of 4-ethyl carboxylate

Table 1
Physicochemical properties of the newly synthesized compounds **21**–**47**.

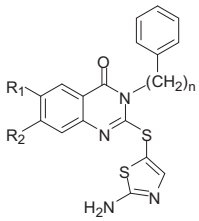

21-26

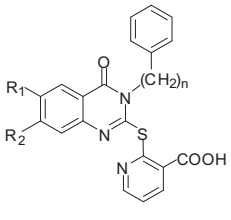

28-33

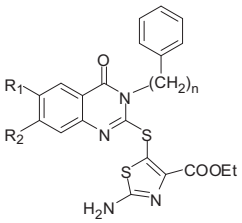

35-40

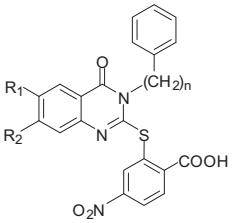

42-47

Compd.	R_1	R_2	*n*	Yield%	M.p., °C	Molecular formulas[a]
21	CH_3	H	0	42	122–5	$C_{18}H_{14}N_4OS_2$
22	CH_3	H	1	25	148–50	$C_{19}H_{16}N_4OS_2$
23	Cl	H	0	56	132–4	$C_{17}H_{11}ClN_4OS_2$
24	Cl	H	1	48	161–3	$C_{18}H_{13}ClN_4OS_2$
25	OCH_3	OCH_3	0	55	144–6	$C_{19}H_{16}N_4O_3S_2$
26	OCH_3	OCH_3	1	30	152–5	$C_{20}H_{18}N_4O_3S_2$
28	CH_3	H	0	49	131–4	$C_{21}H_{15}N_3O_3S$
29	CH_3	H	1	47	138–40	$C_{22}H_{17}N_3O_3S$
30	Cl	H	0	61	121–3	$C_{20}H_{12}ClN_3O_3S$
31	Cl	H	1	23	155–7	$C_{21}H_{14}ClN_3O_3S$
32	OCH_3	OCH_3	0	46	110–2	$C_{22}H_{17}N_3O_5S$
33	OCH_3	OCH_3	1	52	129–31	$C_{23}H_{19}N_3O_5S$
35	CH_3	H	0	44	125–7	$C_{21}H_{18}N_4O_3S_2$
36	CH_3	H	1	63	119–21	$C_{22}H_{20}N_4O_3S_2$
37	Cl	H	0	31	133–5	$C_{20}H_{15}ClN_4O_3S_2$
38	Cl	H	1	37	145–7	$C_{21}H_{17}ClN_4O_3S_2$
39	OCH_3	OCH_3	0	63	124–7	$C_{22}H_{20}N_4O_5S_2$
40	OCH_3	OCH_3	1	49	153–5	$C_{23}H_{22}N_4O_5S_2$
42	CH_3	H	0	22	139–41	$C_{22}H_{15}N_3O_5S$
43	CH_3	H	1	39	154–8	$C_{23}H_{17}N_3O_5S$
44	Cl	H	0	52	114–9	$C_{21}H_{12}ClN_3O_5S$
45	Cl	H	1	43	155–8	$C_{22}H_{14}ClN_3O_5S$
46	OCH_3	OCH_3	0	28	149–51	$C_{23}H_{17}N_3O_7S$
47	OCH_3	OCH_3	1	35	158–61	$C_{24}H_{19}N_3O_7S$

[a] Analyzed for C, H, N; results were within ±0.4% of the theoretical values for the given formulas.

Table 2
DHFR inhibition (IC_{50}, μM), and antimicrobial activity results of compounds **21**–**26**, **28**–**33**.

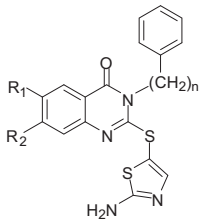

21-26

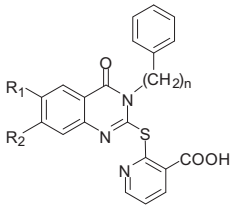

28-33

Compd.	R_1	R_2	*n*	DHFR inhibition (IC_{50}, μM)	*S. aureus*	*B. subtilis*	*M. luteus*	*E. coli*	*P. aeruginosa*
21	CH_3	H	0	0.8	–	–	–	–	–
22	CH_3	H	1	1.0	–	–	–	–	–
23	Cl	H	0	4.0	18 (8.0)	22 (4.0)	14	–	–
24	Cl	H	1	2.0	16	18	–	15	–
25	OCH_3	OCH_3	0	0.5	18 (8.0)	20 (4.0)	16 (4.0)	18 (4.0)	14
26	OCH_3	OCH_3	1	3.0	17	18	–	16	–
28	CH_3	H	0	8.0	20 (4.0)	22 (4.0)	14	16	12
29	CH_3	H	1	10.0	15	16	12	–	–
30	Cl	H	0	8.0	15	16	–	–	–
31	Cl	H	1	10.0	14	18	–	–	–
32	OCH_3	OCH_3	0	7.0	20 (4.0)	22 (4.0)	15	22 (2.0)	–
33	OCH_3	OCH_3	1	5.0	22 (4.0)	26 (2.0)	15	18 (4.0)	12
Gentamicin	–	–	–	Nd	27 (2.0)	25 (2.0)	18 (2.0)	21 (0.5)	19 (1.0)
Sulphacetamide	–	–	–	Nd	20 (2.0)	22 (2.0)	18 (2.0)	28 (1.0)	25 (2.0)

Inhibition zone (mm): (–) not active (8 mm), weak activity (8–12 mm), moderate activity (12–15 mm), strong activity (>15 mm). Solvent: DMSO (8 mm). MICs showed in parentheses. Nd, not determined.

Table 3
DHFR inhibition (IC_{50}, μM), and antimicrobial activity results of compounds **35**–**40**, **42**–**47**.

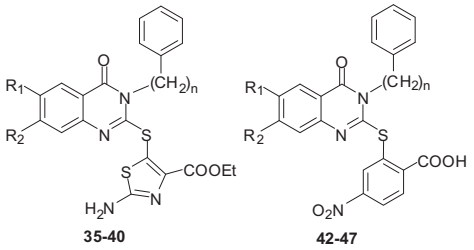

Compd.	R_1	R_2	*n*	DHFR inhibition (IC_{50}, μM)	*S. aureus*	*B. subtilis*	*M. luteus*	*E. coli*	*P. aeruginosa*
35	CH_3	H	0	1.0	24 (2.0)	26 (2.0)	14	18 (4.0)	12
36	CH_3	H	1	4.0	24 (2.0)	26 (2.0)	20 (4.0)	24 (2.0)	18 (4.0)
37	Cl	H	0	3.0	–	–	–	–	–
38	Cl	H	1	1.0	20 (4.0)	22 (2.0)	14	20 (4.0)	–
39	OCH_3	OCH_3	0	0.3	–	–	–	–	–
40	OCH_3	OCH_3	1	2.0	18	20	–	–	–
42	CH_3	H	0	10.0	–	–	–	–	–
43	CH_3	H	1	12.0	–	–	–	–	–
44	Cl	H	0	10.0	14	20 (4.0)	–	–	–
45	Cl	H	1	8.0	–	15	–	–	–
46	OCH_3	OCH_3	0	10.0	18 (8.0)	20 (4.0)	–	22 (2.0)	–
47	OCH_3	OCH_3	1	3.0	18	–	–	–	–
Gentamicin	–	–	–	Nd	27 (2.0)	25 (2.0)	18 (2.0)	21 (0.5)	19 (1.0)
Sulphacetamide	–	–	–	Nd	20 (2.0)	22 (2.0)	18 (2.0)	28 (1.0)	25 (2.0)

Inhibition zone (mm): (–) not active (8 mm), weak activity (8–12 mm), moderate activity (12–15 mm), strong activity (>15 mm). Solvent: DMSO (8 mm). MICs showed in parentheses. Nd, not determined.

to the thiazole function of **21** produced the equipotent derivatives **22** and **35** (IC_{50} 1.0 μM); the introduction of 4-ethyl carboxylate to the thiazole function of **22** (IC_{50} 4.0 μM) produced **36** with four fold decrease in DHFR inhibition activity. Replacing of the thiazole moiety of **21** by either 2-nicotinic acid or 4-nitrobenzoic acid functions yielded compounds **28**, **29**, **42**, **43** with almost 10 fold decrease in potency. In the 6-chloro series, the presence of 3-phenyl and 2-aminothiazole-5-thiol produced **23** with IC_{50} 4.0 μM; replacing the 3-phenyl function by 3-benzyl or the introduction of 4-ethyl carboxylate to the thiazole moiety of **23** produced derivatives **24** and **37** (IC_{50} 2.0 and 3.0 μM, respectively); the introduction of 4-ethyl carboxylate to the thiazole function of **24** (IC_{50} 4.0 μM) produced **38** with two fold increase in DHFR inhibition activity. Replacing of the thiazole moiety of **23** by either 2-nicotinic acid or 4-nitrobenzoic acid functions yielded compounds **30**, **31**, **44**, **45** with almost two fold decrease in potency. In the 6,7-dimethoxy series, the presence of 3-phenyl and 2-aminothiazole-5-thiol produced **25** with IC_{50} 0.5 μM; replacing of the 3-phenyl of **25** by 3-benzyl function produced **26** (IC_{50} 3.0 μM) with six fold decrease in DHFR inhibition activity. The introduction of 4-ethyl carboxylate to the thiazole moiety of **25** yielded **39** (IC_{50} 0.3 μM) the most potent DHFR inhibitor in this study. Replacing of the thiazole moiety of **25** by either 2-nicotinic acid or 4-nitrobenzoic acid functions yielded compounds **32**, **33**, **46**, **47** with almost 6–20 fold decrease in potency. In general, the type of substituent at positions 2-, 3-, and 6- of the quinazoline nucleus proved to manipulate and contribute to the DHFR inhibition activity in the following order: 2-thiazolethio- > 2-pyridinethio- > 2-phenylthio-; 3-phenyl- > 3-benzyl-; and 6,7-dimethoxy- > 6-methyl- > 6-chloro-.

2.3. Antimicrobial activity

The synthesized compounds (**21**–**47**) were tested for their *in vitro* antimicrobial activity against a panel of standard strains of Gram-positive bacteria (*Staphylococcus aureus*, *Bacillus subtilis* and *Micrococcus luteus*), and Gram-negative bacteria (*Escherichia coli* and *Pseudomonas aeruginosa*). The primary screen was carried out using the agar disc-diffusion method [35,36]. The antibiotics gentamicin (100 μg/disc), and the DHFR inhibitor sulphacetamide (100 μg/disc) were used as positive controls. The obtained results revealed that the tested compounds expressed varying degrees of activity against the tested microorganisms (Tables 2 and 3). Strong activity (>15 mm inhibition zone) against the Gram-positive bacteria was observed for compounds **23**–**28**, **32**, **33**, **35**, **36**, **38**, **40**, **46** and **47** against *S. aureus*; **23**–**33**, **35**, **36**, **38**, **40**, **44**, and **46** against *B. subtilis*, and **25** and **36** against *M. luteus*. In case of Gram-negative bacteria, strong activity was observed for compounds **25**–**27**, **32**, **33**, **35**, **36**, **38** and **46** against *E. coli*. Compounds **25**, **28**, **33**, **35**, and **36** showed a remarkable broad-spectrum activity against both Gram-positive and Gram-negative bacteria. Compounds **23**, **29**–**31**, **40**, **44** appeared to be selective and active against Gram-positive bacteria. The minimal inhibitory concentrations (MICs) for the most active compounds was carried out using the micro-dilution susceptibility method as shown in Tables 2 and 3. The Gram-positive bacteria *B. subtilis* and *S. aureus* are sensitive to majority of the tested compounds. Comparing the potency of the active antibacterial compounds and their DHFR inhibition revealed that compounds **25**, **35** and **38** might exert their activity through DHFR inhibition.

2.4. Antitumor screening

The synthesized compounds **21**–**47** were subjected to the National Cancer Institute (NCI) *in vitro* disease-oriented human cells screening panel assay for *in vitro* antitumor activity. A single dose (10 μM) of the test compounds were used in the full NCI 60 cell lines panel assay which includes nine tumor subpanels namely; Leukemia, Non-small cell lung, Colon, CNS, Melanoma, Ovarian, Renal, Prostate, and Breast cancer cells [30–33]. The data reported as mean-graph of the percent growth of the treated cells, and presented as percentage growth inhibition (GI%) caused by the test compounds. Only compound **29** showed broad spectrum potency

toward several tumor cell lines with GI values range of 25.8–41.2%. Concerning activity toward individual cell lines, leukemia SR cell line showed sensitivity toward compounds **21**, **23**, **31** and **33** with GI values of 37.8, 29.1, 32.8 and 29.8%, respectively; also CAKI-1 renal cancer cell line toward **22**, **24**, **26**, **29** and **31** with GI values of 30.3, 25.6, 25.4, 41.2 and 30.3%, respectively; while PC-3 prostate cancer cell line toward **24**, **29** and **31** with GI values of 28.2, 32.8 and 25.2%, respectively (Table 4).

3. Molecular dynamic study

The investigated quinazolines were subjected to molecular modeling study to evaluate their recognition profile at DHFR binding-pocket, in comparison to the dihydrofolate inhibitor 2,4-diamino-6-[*N*-(2′,5′-dimethoxybenzyl)-*N*-methylamino]quinazoline (COQ). The tertiary complex of DHFR, NADPH and COQ was used as a reference for modeling and docking [37–42]. At DHFR pocket, COQ formed bifurcated H-bonding with the key residue Glu32 and Ile10 [43–46], (Fig. 1). Molecular dynamic study indicated that the tested quinazoline's recognition with the key amino acid Arg38 and Lys31 is essential for binding and biological activity. The amino acid Lys31 is not one of the key residues of the recognition of the parent ligand COQ but it plays a crucial role in the recognition of the tested compounds. Fig. 1 showed the binding mode and residues involved in the recognition of the most active compound **39** (IC_{50} 0.3 μM), and the most inactive compound **43** (IC_{50} 12.0 μM) docked and minimized in the DHFR binding pocket.

The aligned binding conformations of **39** revealed a clear preference for binding where the compound occupies the site quite well as seen in Fig. 2. Compound **39** occupies a space deep in the cavity and the ester tail extends toward the solvent showing a strong hydrophobic interaction with the hydrophobic residues in the DHFR active site. The presence of the 2-amino function at the thiazole moiety of **39** as a hydrogen bond donor is important for DHFR inhibition activity that is in contrary to the least active compound **43** which lacks such association and functional group. In addition, N1 and 4-carbonyl moieties of the quinazoline ring performed hydrogen bonding with the backbone amino acids of the active site. Compound **39** is involved also in van der Waals interactions through its phenyl ring with Ala126 and Phe36. (Residue was not shown in Fig. 2 for clarity.) Meanwhile, compound **43** did not interact with any amino acid in the active site indicating that the ligand in question projects out of the active site, this might be attributed to either the ligand atoms and the remaining surface area are outside of the binding pocket, or they are in an interior region with difficult or practically no distinct binding.

To probe similarity between the 3D structures of the most active compounds **25** and **39**, flexible alignment was employed. Our initial approach was to employ MOE/MMFF94 flexible alignment to automatically generate superposition of the compounds under investigation with minimal user bias [47]. 200 conformers of each compound were generated and minimized with a distance-dependant dielectric model. A low energy set of 100 was selected for further analysis. The top scoring alignment of both the least

Table 4
Percentage growth inhibition (GI%) of *in vitro* subpanel tumor cell lines at 10 μM concentration of compounds **21**–**33**.

Subpanel tumor cell lines[a]	**21**	**22**	**23**	**24**	**25**	**26**	**28**	**29**	**30**	**31**	**32**	**33**
Leukemia												
CCRF-CEM	–	–	–	13.7	–	22.8	–	16.5	–	17.8	–	–
HL-60(TB)	–	–	–	–	–	–	–	–	–	–	–	13.2
MOLT-4	–	–	–	16.8	–	–	–	15.3	–	16.7	–	13.8
RPMI-8226	–	16.8	–	18.9	12.5	15.9	10.4	25.8	–	16.3	–	12.5
SR	37.8	–	29.1	–	14.8	–	–	14.4	–	32.8	–	29.8
Non-small cell lung cancer												
A549/ATCC	–	–	–	–	–	–	–	–	–	–	–	–
EKVX	–	25.9	12.9	11.9	12.7	16.1	–	26.6	–	25.4	–	23.1
NCI-H226	12.4	19.9	25.7	17.1	–	10.4	–	21.2	15.1	18.4	12.0	14.0
NCI-H23	–	–	10.9	–	–	–	–	–	–	–	–	–
NCI-H522	13.8	–	14.0	16.0	–	19.8	–	24.4	–	13.1	11.4	17.3
CNS cancer												
SF-295	–	17.3	–	16.6	–	–	–	14.2	–	15.7	–	–
SNB-19	–	–	–	–	–	–	–	14.2	–	–	–	–
SNB-75	–	20.4	–	10.7	–	13.3	–	30.0	–	18.4	–	–
Melanoma												
LOX IMVI	–	10.4	11.2	14.9	–	10.8	–	13.8	–	13.6	–	–
MALME-3M	–	12.3	–	10.8	–	–	–	–	–	–	–	–
MDA-MB-435	–	–	–	–	–	–	–	21.8	–	–	–	–
SK-MEL-5	–	–	–	–	–	12.9	–	14.4	–	–	–	–
UACC-62	–	12.2	–	14.4	–	–	–	30.4	–	16.7	–	11.6
Ovarian cancer												
IGORV1	14.3	21.8	–	12.0	13.0	–	–	16.3	–	14.7	–	–
OVCAR-4	–	–	–	13.8	–	–	–	16.2	–	20.6	–	14.3
NCI/ADR-RES	–	–	–	–	–	–	–	12.7	–	–	–	–
Renal cancer												
A498	–	–	–	11.2	–	–	–	11.4	–	–	–	–
CAKI-1	20.9	30.3	24.1	25.6	17.8	25.4	13.1	41.2	–	30.3	17.7	15.9
RXF 393	–	–	–	–	–	–	–	21.5	–	–	–	–
SN12C	–	–	–	–	–	–	–	11.2	–	–	–	–
UO-31	20.7	29.4	–	14.8	22.2	17.4	12.1	20.6	20.5	20.3	12.0	14.6
Prostate cancer												
PC-3	10.1	22.6	10.2	28.2	12.0	22.4	11.7	32.8	–	25.2	–	–
Breast cancer												
MCF7	–	10.8	19.0	–	–	–	–	16.6	–	–	–	13.5
MDA-MB-231/ATCC	18.1	15.2	21.5	11.2	18.6	19.1	–	30.5	10.4	24.7	–	–
HS 578T	–	–	–	–	–	–	–	12.5	–	–	–	–
T-47D	–	–	19.1	10.4	–	–	–	–	15.0	14.1	–	–

[a] –, GI < 10%; nt, not tested.

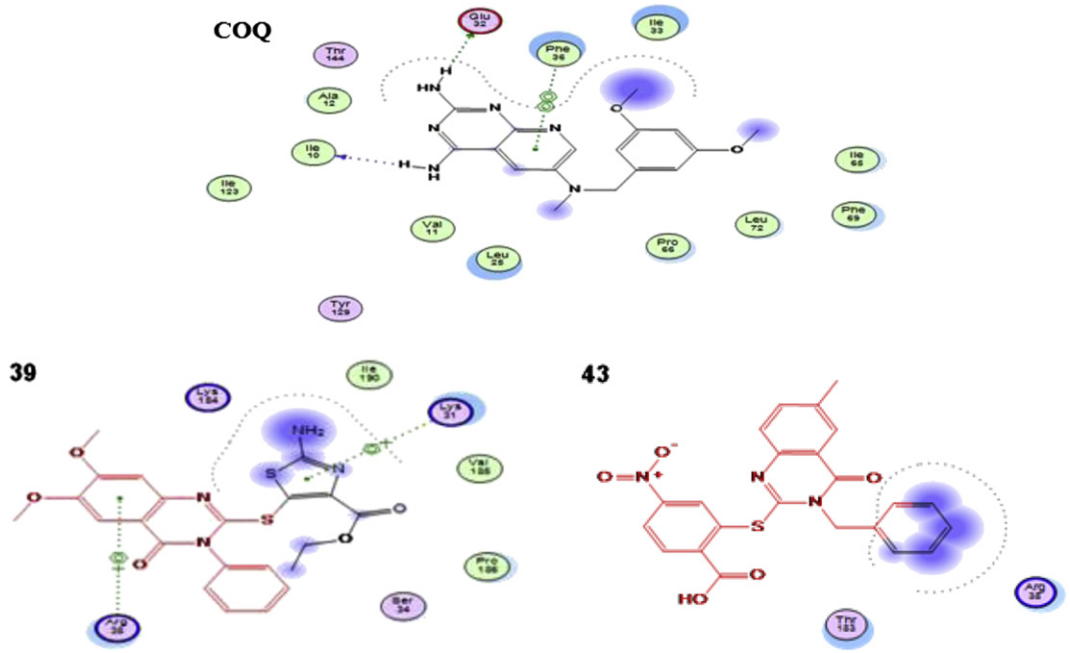

Fig. 1. The binding mode and residues involved in the recognition for COQ, the most active compound **39** (IC_{50} 0.3 μM) and the most inactive compound **43** (IC_{50} 12.0 μM) docked and minimized in the DHFR binding pocket.

strain energy and the best alignment score is shown in Fig. 3. The most active compounds **25** and **39** align completely (Fig. 3a), also the least active compounds **29**, **42**, and **43** align perfectly (Fig. 3b); while compounds **39**, **42** and **43** showed a dramatic deviation from alignment (Fig. 3c). Examination of the flexible alignment results of the active versus the inactive DHFR inhibitors in this study revealed that the inactive compounds **42** and **43** were aligned in a distinct different pattern from that of the most active compound **39** (Fig. 3c). Flexible alignment projected the importance of the 2-aminothiazole moiety of **39** as a five membered ring bearing basic center for activity; and the pyridine-2-carboxylic acid (**28**–**33**) or 4-nitrobenzoic acid (**42**–**47**) functions as a six membered ring bearing acidic center for the diminished potency. This evidence is supported by the DHFR inhibition data displayed in Tables 2 and 3.

Atomic-level details of the structure of pharmaceutically relevant receptors are not available; in such cases, 3D superposition of putative ligands can be used to deduce specific structural requirements for biological activity [47,48]. Structure superposition of the most active compounds **21**, **25** and **39** (Fig. 4) with mark points such as *N*-1 of the quinazoline nucleus, the thiazole ring, the 3-phenyl fragment, 2-S-linkage directly attached to quinazoline moiety, 2-amino group at the thiazole function and the π-system represented by aryl group of the quinazoline core, align fairly well with almost complete superposition of the quinazoline rings (0.4 Å). This superposition suggests the possible existence of a region on the receptor suited for specific recognition of such features. This hypothesis is supported by biological results which strongly suggest that these seven chosen mark points could be used as a pharmacophore model for further optimization.

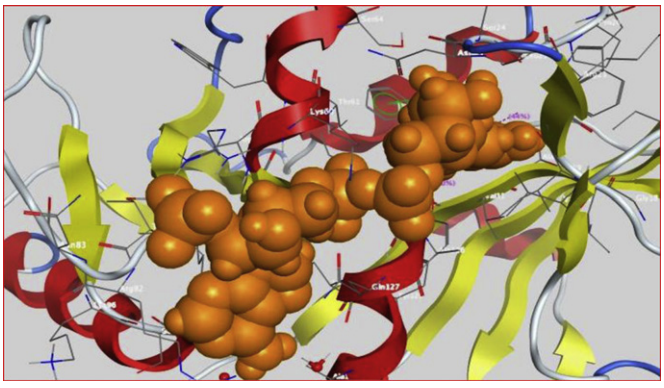

Fig. 2. The aligned conformation of compound 39 (IC_{50} 0.3 μM) in the DHFR binding pocket.

As an attempt to investigate the reasons behind the diminished DHFR inhibition activity of **29**, **42** and **43**, electrostatic mapping was carried out for the lowest energy conformer of compound **43**, to examine the similarity and dissimilarity in the electronic and electrostatic binding characteristics of the molecule surface and the conformational properties, in comparison to the most active compound **39**. Fig. 5 showed some common features of **39**, which are negative charged hydrogen bond acceptor–donor region located on the 4-carbonyl and N-1; a non-polar area located on the aryl moiety attached to the quinazoline core distributed on both sides of the aryl parts; and hydrophilic region located on 4-carbonyl, N-1 of the quinazoline core. Such results indicated the structure and hence biological similarity among those active analogs. On the contrary, the low activity of the other compounds, represented by **43** may be attributed to the difference in electrostatic mapping in which the hydrogen bond area was mainly located on the carboxylic group. Similarly, hydrophobic surface mapping study of the most active compound **39** (Fig. 6a) pointed out the hydrophobic region which is responsible for the interaction with the key amino acid residues inside the enzyme active pocket. On the other hand, the hydrophobic distributions of the least active compound **43** (Fig. 6b) lack such hydrophobic moieties and hence the required lipophilicity, instead a hydrophilic region was located on the carboxylic acid fragment. The obtained charge distribution, electrostatic, hydrophobic mapping and conformation of the active agents suggest a distinct different interaction of the active and inactive molecules with the potential protein-binding site.

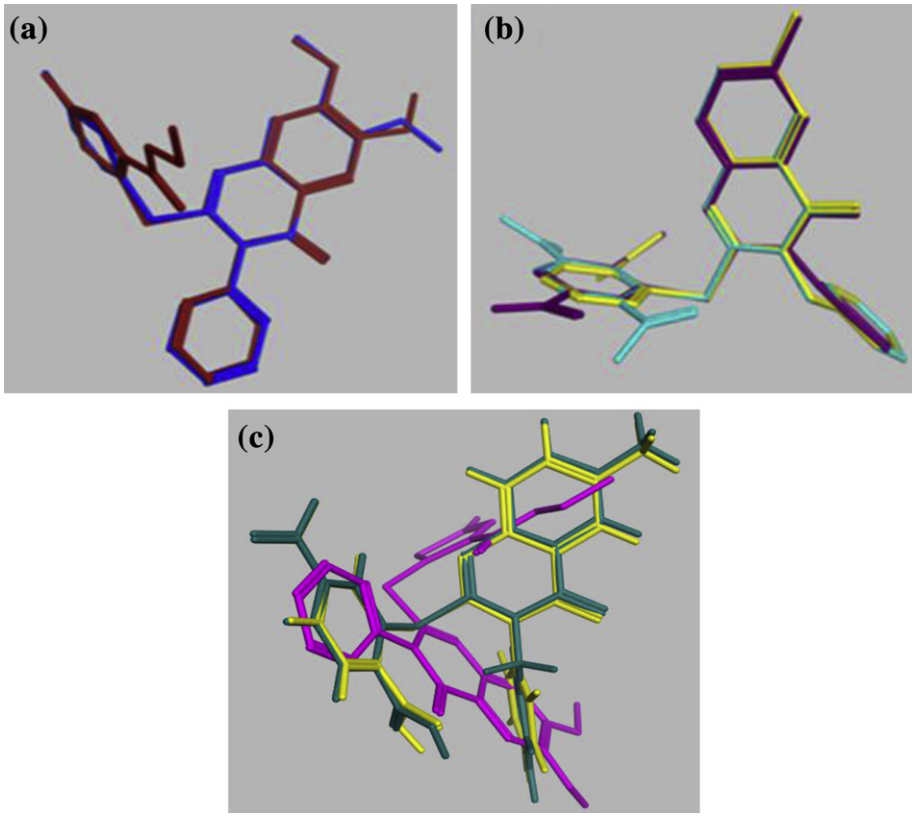

Fig. 3. (a) Flexible alignment of the most active compounds **25** (blue), and **39** (red). (b) Flexible alignment of the least active compounds **29** (yellow), **42** (violet), and **43** (cyan). (c) Flexible alignment of the most active compound **39** (pink) against the least active compounds **42** (yellow) and **43** (cyan). (For interpretation of the references to colour in this figure legend, the reader is referred to the web version of this article.)

4. Conclusion

Compounds **21**, **22**, **25**, **35**, **38**, and **39** proved to be the most active DHFR inhibitors with IC_{50} range of 0.3–1.0 μM. Structure activity relationship studies revealed that, the type of substituent at positions 2-, 3- and 6- of the studied quinazolin-4-ones manipulate the DHFR inhibition activity. In general, the 2-thiazolethio-substituent on the quinazoline nucleus contributed to the DHFR inhibition activity more than the 2-phenylthio- or the 2-pyridinethio-moieties; also 3-phenyl-, and 6,7-dimethoxy substituent favor the activity rather than 3-benzyl-, 6-methyl or 6-chloro functions. Compounds **25**, **28**, **33**, **35**, and **36** showed a remarkable broad-spectrum activity against both Gram-positive and Gram-negative bacteria. Compounds **25**, **35** and **38** might exert their activity through DHFR inhibition. Meanwhile, compound **29** showed broad spectrum potency toward several tumor cell lines with GI values range of 25.8–41.2%. Molecular modeling study was performed and concluded that recognition with key amino acid Arg38 and Lys31 is essential for binding and biological activities of the investigated quinazolines. Flexible alignment; electrostatic and hydrophobic mappings were also performed. This model justifies the importance of the main pharmacophoric groups (the 4-carbonyl fragment, the basic nitrogen atom at N-1, and the hydrophobic π-system regions). The substitution pattern and spatial considerations of the π-systems in regard to the quinazoline nucleus proved to be critical for biological activity. Therefore, the obtained model could be useful for the development of new DHFR inhibitors.

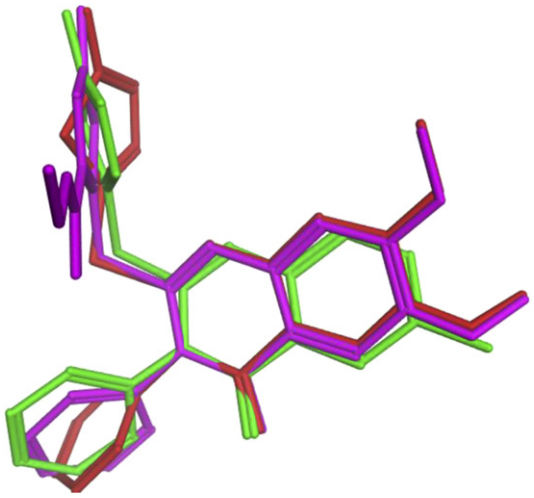

Fig. 4. Electrostatic and hydrophobic map of the lowest energy conformers for the most active compound **39** and the least active compound **43**, maps are color coded: red for a hydrogen bond and a hydrophilic region, and green for a hydrophobic region. (For interpretation of the references to colour in this figure legend, the reader is referred to the web version of this article.)

5. Experimental part

Melting points (°C) were determined on Mettler FP80 melting point apparatus and are uncorrected. Microanalyses were performed on a Perkin–Elmer 240 elemental analyzer at the Central Research Laboratory, College of Pharmacy, King Saud University. All of the new compounds were analyzed for C, H and N and agreed

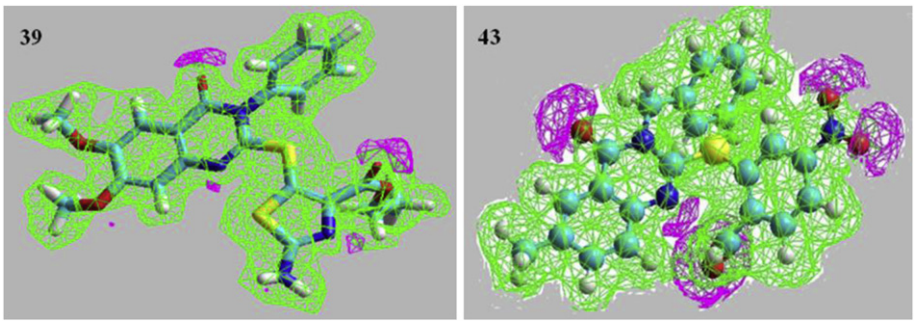

Fig. 5. Electrostatic maps of the lowest energy conformers for the most active compound **39** and the least active compound **43**. Red for a hydrogen bond and a hydrophilic region, and green for a hydrophobic region. (For interpretation of the references to colour in this figure legend, the reader is referred to the web version of this article.)

with the proposed structures within ±0.4% of the theoretical values. ^{1}H, ^{13}C NMR spectra were recorded on a Bruker 500 MHz FT spectrometer (the Central Research Laboratory, College of Pharmacy, King Saud University); chemical shifts are expressed in δ ppm with reference to TMS. Mass spectral (MS) data were obtained on a Perkin Elmer, Clarus 600 GC/MS and Joel JMS-AX 500 mass spectrometers. Thin layer chromatography was performed on precoated (0.25 mm) silica gel GF_{254} plates (E. Merck, Germany), compounds were detected with 254 nm UV lamp. Silica gel (60–230 mesh) was employed for routine column chromatography separations. DHFR inhibition activity experiments were performed at Pharmacology Department, College of Pharmacy, King Saud University. Bovine liver DHFR enzyme, methotrexate (MIX) was used in the assay (Sigma Chemical Co, USA). The *in vitro* antimicrobial testing was performed at Department of Microbiology, Faculty of Pharmacy, Mansoura University, Egypt. The agar disc-diffusion method and a panel of standard strains (*S. aureus* IFO 3060, *B. subtilis* IFO 3007, *M. luteus* IFO 3232, *E. coli* IFO 3301, and *P. aeruginosa* IFO 3448) were employed. *In vitro* antitumor activity was conducted at the NCI, Bethesda, MD. All modeling experiments were conducted with Hyperchem 8.0.5 package from Hypercube running on a PC computer. The docking of the candidates into DHFR pocket was performed with MOE software. Starting coordinate of DHFR enzyme in tertiary complex with reduced-nicotinamide adenine dinucleotide phosphate (NADPH) and COQ, code ID 1LY4, was obtained from the Protein Data Bank. Compounds **14**–**19** were previously reported [24–26].

5.1. Chemistry

5.1.1. 2-(2-Aminothiazol-5-ylthio)-3-phenyl or benzyl-6-substituted-quinazolin-4(3H)-ones (**21**–**24**)

A mixture of 2-amino-5-bromothiazole (**20**, 1.79 g, 0.01 mol), the appropriate 2-thioxo-quinazoline analogs (**14**–**17**, 0.01 mol), anhydrous potassium carbonate (1.5 g, 0.01 mol) in DMF (10 ml) was heated under reflux for 14 h. Solvent was then removed under reduced pressure. The obtained residue was dissolved in CH_2Cl_2, then washed the organic layer several times with water, and finally dried. The obtained solid was recrystallized from ethanol to obtain compounds **21**–**24**, (Table 1). **21**: ^{1}H NMR (DMSO-d_6) δ 2.26 (s, 3H, CH_3), 3.77 (brs, 2H, NH_2), 7.00 (d, 1H, J = 8 Hz, Ar–H), 7.14 (d, 2H, J = 8.5 Hz, Ar–H), 7.39 (t, 1H, J = 7.5 Hz, Ar–H), 7.46 (t, 2H, J = 7.5 Hz, Ar–H), 7.53 (d, 1H, J = 7 Hz, Ar–H), 7.79 (s, 1H, Ar–H), 7.96 (s, 1H, thiazole–H). ^{13}C NMR δ 20.2, 115.2, 115.7, 116.0, 127.0, 128.8, 129.0, 133.9, 135.8, 136.6, 137.6, 139.4, 150.1, 159.8, 162.2, 175.5. MS m/z (%): 367 (2.5, M^+). **22**: ^{1}H NMR (DMSO-d_6) δ 2.34 (s, 3H, CH_3), 3.45 (brs, 2H, NH_2), 5.09 (s 2H, benzylic–H), 7.11 (d, 1H, J = 8.5 Hz, Ar–H), 7.23 (d, 2H, J = 4.5 Hz, Ar–H), 7.31 (t, 1H, J = 4 Hz, Ar–H), 7.50 (t, 2H, J = 7 Hz, Ar–H), 7.61 (d, 1H, J = 7.5 Hz, Ar–H), 7.77 (s, 1H, Ar–H), 7.99 (s, 1H, thiazole–H). ^{13}C NMR δ 20.4, 43.1, 113.5, 115.2, 115.7, 126.7, 127.4, 128.2, 131.9, 134.2, 136.2, 136.7, 137.3, 137.4, 150.1, 161.9, 175.0. MS m/z (%): 380 (1.2, M^+). **23**: ^{1}H NMR (DMSO-d_6) δ 7.28 (t, 2H, J = 8 Hz, Ar–H), 7.33 (t, 1H, J = 7 Hz, Ar–H), 7.42 (d, 2H, J = 7.5 Hz, Ar–H), 7.49 (d, 2H, J = 2.5 Hz, Ar–H), 7.83 (d, 1H, J = 2.5 Hz, Ar–H), 7.89 (s, 1H, thiazole–H), 13.15 (s, 2H, NH_2). ^{13}C NMR δ 115.8, 117.7, 117.9, 126.4, 128.1, 128.9, 134.9, 135.5, 138.4, 139.1, 149.9, 158.8, 161.2, 176.1, 206.3. MS m/z (%): 386 (24.3, M^+). **24**: ^{1}H NMR (DMSO-d_6) δ 5.10 (s, 2H, benzylic–H), 7.19 (d, 1H, J = 7.5 Hz, Ar–H), 7.26 (t, 2H, J = 8 Hz, Ar–H), 7.34 (t, 1H, J = 7.5 Hz, Ar–H), 7.48 (d, 2H, J = 8.5 Hz, Ar–H), 7.59 (d, 1H, J = 7 Hz, Ar–H), 8.63 (s, 1H, thiazole–H), 8.72 (s, 1H, Ar–H). 13.53 (s, 2H, NH_2). ^{13}C NMR δ 113.9, 116.7, 117.3, 123.7, 127.5, 128.3, 135.9, 136.8, 142.0, 143.0, 143.1, 144.3, 149.9, 158.6, 160.9, 176.5. MS m/z (%): 400 (1.6, M^+).

5.1.2. 2-(2-Aminothiazol-5-ylthio)-6,7-dimethoxy-3-phenyl or benzyl-quinazolin-4(3H)-ones (**25**, **26**)

A mixture of 2-amino-5-bromothiazole (**20**, 1.79 g, 0.01 mol), the appropriate 2-thioxo-quinazoline analogs (**18** or **19**, 0.01 mol),

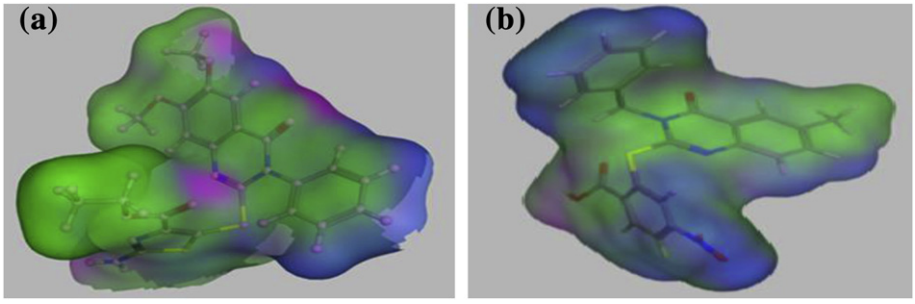

Fig. 6. (a) Surface map for the most active compound **39** in pocket side. (b) Surface map for the least active compound **43**. Pink hydrogen bond, blue mild polar, green hydrophobic. (For interpretation of the references to colour in this figure legend, the reader is referred to the web version of this article.)

anhydrous potassium carbonate (1.5 g, 0.01 mol) in DMF (10 ml) was heated under reflux for 14 h. Solvent was then removed under reduced pressure and continued as mentioned under compounds **21**–**24** (Table 1). **25**: ^{1}H NMR (DMSO-d_6) δ 2.89 (brs, 2H, NH_2), 4.35 (s, 6H, OCH_3), 7.31 (d, 2H, J = 8 Hz, Ar–H), 7.42 (t, 1H, J = 7.5 Hz, Ar–H), 7.51 (t, 2H, J = 8 Hz, Ar–H), 7.96 (s, 1H, thiazole–H), 8.52 (s, 2H, Ar–H). ^{13}C NMR δ 55.2, 55.9, 114.6, 116.5, 117.1, 123.5, 128.4, 129.1, 135.1, 138.8, 141.9, 142.8, 143.5, 144.6, 149.9, 161.1, 177.1. MS m/z (%): 412 (3.0, M^+). **26**: ^{1}H NMR (DMSO-d_6) δ 3.42 (brs, 2H, NH_2), 3.85 (s, 6H, OCH_3), 5.19 (s, 2H, benzylic–H), 6.74 (s, 2H, Ar–H), 7.04–7.39 (m, 5H, Ar–H), 7.96 (s, 1H, thiazole–H). ^{13}C NMR δ 34.1, 46.5, 55.7, 56, 105.6, 105.9, 106.9, 111.4, 126.7, 127.3, 127.5, 128.1, 135.9, 143.3, 155.0, 155.5, 161.4, 177.2. MS m/z (%): 426 (5.1, M^+).

5.1.3. 2-(3-Phenyl or benzyl-6-substituted-4-oxo-3,4-dihydro quinazoline-2-ylthio)nicotinic acid derivatives (**28**–**31**)

A mixture of 2-chloronicotinic acid (**27**, 1.57 g, 0.01 mol), the appropriate 2-thioxo-quinazoline analogs (**14**–**17**, 0.01 mol), anhydrous potassium carbonate (1.5 g, 0.01 mol) in DMF (10 ml) was heated under reflux for 24 h. Solvent was then removed under reduced pressure and continued as mentioned under compounds **21**–**24** (Table 1). **28**: ^{1}H NMR (DMSO-d_6) δ 2.85 (s, 3H, CH_3), 7.15 (d, 1H, J = 8 Hz, Ar–H), 7.26 (d, 2H, J = 7.5 Hz, Ar–H), 7.31 (d, 1H, J = 7 Hz, Ar–H), 7.36 (d, 1H, J = 8 Hz, Ar–H), 7.41 (d, 1H, J = 7.5 Hz, Ar–H), 7.48 (t, 2H, J = 7.5 Hz, Ar–H), 7.52 (d, 1H, J = 7 Hz, Ar–H), 7.62 (d, 1H, J = 7 Hz, Ar–H), 7.76 (s, 1H, Ar–H), 13.0 (s, 1H, COOH). ^{13}C NMR δ 20.4, 115.7, 116.1, 126.7, 128.1, 128.7, 128.9, 129.0, 133.9, 136.6, 137.6, 137.6, 139.4, 141.2, 143.2, 144.5, 159.8, 161.3, 175.5. MS m/z (%): 389 (0.2, M^+). **29**: ^{1}H NMR (DMSO-d_6) δ 2.37 (s, 3H, CH_3), 5.68 (s, 2H, benzylic–H), 7.11 (s, 1H, Ar–H), 7.24 (d, 2H, J = 6 Hz, Ar–H), 7.31–7.35 (m, 5H, Ar–H), 7.50 (d, 1H, J = 7.5 Hz, Ar–H), 7.60 (d, 1H, J = 7.5 Hz, Ar–H), 7.76 (t, 1H, J = 8.5 Hz, Ar–H), 13.01 (s, 1H, COOH). ^{13}C NMR δ 20.4, 62.9, 115.3, 115.7, 126.7, 126.9, 127.1, 127.4, 128.2, 128.3, 129.4, 129.9, 131.5, 134.2, 136.6, 136.7, 137.1, 156.4, 162.5, 175.0. MS m/z (%): 403 (1.0, M^+). **30**: ^{1}H NMR (DMSO-d_6) δ 7.28 (d, 2H, J = 7 Hz, Ar–H), 7.34 (d, 2H, J = Hz, Ar–H), 7.43 (d, 2H, J = 7.5 Hz, Ar–H), 7.49 (t, 3H, J = 10 Hz, Ar–H), 7.84 (d, 1H, J = 2.5 Hz, Ar–H), 7.89 (d, 1H, J = 2 Hz, Ar–H), 13.15 (s, 1H, COOH). ^{13}C NMR δ 117.4, 117.7, 117.9, 126.2, 126.4, 128.1, 128.7, 128.8, 128.9, 134.9, 135.4, 138.4, 138.7, 139.1, 149.9, 158.8, 161.2, 176.1. MS m/z (%): 410 (2.2, M^+). **31**: ^{1}H NMR (DMSO-d_6) δ 5.66 (s, 2H, benzylic–H), 7.24 (t, 2H, J = 14 Hz, Ar–H), 7.25–7.28 (m, 4H, Ar–H), 7.44 (d, 2H, J = 8.5 Hz, Ar–H), 7.81 (d, 1H, J = 2.5 Hz, Ar–H), 7.83 (d, 1H, J = 2 Hz, Ar–H), 7.91 (s, 1H, Ar–H), 13.19 (s, 1H, COOH). ^{13}C NMR δ 116.5, 116.8, 117.5, 117.8, 118.0, 119.3, 120.1, 126.3, 126.9, 127.1, 127.5, 128.2, 128.3, 128.4, 135.6, 136.3, 138.0, 158.5, 175.5. MS m/z (%): 423 (9.7, M^+).

5.1.4. 2-(6,7-Dimethoxy-3-phenyl or benzyl-4-oxo-3,4-dihydro quinazoline-2-ylthio)nicotinic acid derivatives (**32**, **33**)

A mixture of 2-chloronicotinic acid (**27**, 1.57 g, 0.01 mol), the appropriate 2-thioxo-quinazoline analogs (**18** or **19**, 0.01 mol), anhydrous potassium carbonate (1.5 g, 0.01 mol) in DMF (10 ml) was heated under reflux for 24 h. Solvent was then removed under reduced pressure and continued as mentioned under compounds **21**–**24** (Table 1). **32**: ^{1}H NMR (DMSO-d_6) δ 3.84 (s, 6H, CH_3O), 6.72 (s, 1H, Ar–H), 6.93 (s, 1H, Ar–H), 7.25 (t, 1H, J = 8 Hz, Ar–H), 7.30–7.32 (m, 7H, Ar–H), 11.28 (s, 1H, COOH). MS m/z (%): 435 (0.5, M^+). **33**: ^{1}H NMR (DMSO-d_6) δ 3.83 (s, 6H, CH_3O), 5.67 (s, 2H, benzylic–H), 6.71 (s, 1H, Ar–H), 6.97 (s, 3H, Ar–H), 7.23–7.31 (m, 6H, Ar–H), 12.89 (s, 1H, COOH). ^{13}C NMR δ 48.5, 55.8, 56, 97.8, 106.8, 108, 126.9, 127.1, 127.4, 128.2, 128.3, 129.5, 129.9, 130.5, 131, 135.1, 136.8, 146.8, 155.4, 158.9, 174.4. MS m/z (%): 449 (5.7, M^+).

5.1.5. Ethyl 2-amino-5-[(3-phenyl or benzyl)-6-substituted-4-oxo-3,4-dihydroquinazolin-2-ylthio)]thiazole-4-carboxylate

A mixture of 2-amino-5-bromothiazole-4-carboxylate (**34**, 2.22 g, 0.01 mol), the appropriate 2-thioxo-quinazoline analogs (**14**–**17**, 0.01 mol), anhydrous potassium carbonate (1.5 g, 0.01 mol) in DMF (10 ml) was heated under reflux for 14–16 h. Solvent was then removed under reduced pressure and continued as mentioned under compounds **21**–**24** (Table 1). **35**: ^{1}H NMR (DMSO-d_6) δ 1.12 (s, 3H, CH_3), 1.29 (t, 3H, J = 13.5 Hz, CH_2CH_3), 3.22–3.25 (q, 2H, CH_2CH_3), 4.28 (s, 2H, NH_2), 7.35 (d, 2H, J = 8 Hz, Ar–H), 7.44 (s, 1H, Ar–H), 7.62 (t, 3H, J = 7.5 Hz, Ar–H), 7.99 (d, 2H, J = 8.5 Hz, Ar–H). MS m/z (%): 438 (2.1, M^+). **36**: ^{1}H NMR (DMSO-d_6) δ 1.15 (s, 3H, CH_3), 1.32 (t, 3H, J = 14 Hz, CH_2CH_3), 3.20–3.24 (q, 2H, CH_2CH_3), 5.49 (s, 2H, benzylic–H), 7.24 (s, 1H, Ar–H), 7.39 (d, 2H, J = 8.5 Hz, Ar–H), 7.58 (t, 3H, J = 8 Hz, Ar–H), 8.22 (d, 2H, J = 7.5 Hz, Ar–H), 13.15 (s, 2H, NH_2). MS m/z (%): 452 (1.2, M^+). **37**: ^{1}H NMR (DMSO-d_6) δ 1.27 (t, 3H, J = 14.5 Hz, CH_2CH_3), 3.12–3.14 (q, 2H, CH_2CH_3), 7.28 (d, 2H, J = 7.5 Hz, Ar–H), 7.57 (t, 2H, J = 8 Hz, Ar–H), 7.75 (d, 2H, J = 2 Hz, Ar–H), 7.85 (d, 1H, J = 2 Hz, Ar–H), 8.14 (d, 1H, J = 2 Hz, Ar–H), 13.16 (s, 2H, NH_2). ^{13}C NMR δ 117.4, 117.9, 125.4, 126.4, 127.4, 128.8, 129.3, 129.5, 129.6, 131.7, 134.7, 135.1, 135.5, 138.4, 139.1, 146.5, 158.9, 176.1. MS m/z (%): 459 (0.9, M^+). **38**: ^{1}H NMR (DMSO-d_6) δ 1.33 (t, 3H, J = 14.5 Hz, CH_2CH_3), 3.23–3.24 (q, 2H, CH_2CH_3), 5.21 (s, 2H, NH_2), 5.65 (s, 2H, benzylic–H), 7.24 (t, 1H, J = 7 Hz, Ar–H), 7.30–7.34 (m, 4H, Ar–H), 7.45 (d, 1H, J = 9 Hz, Ar–H), 7.83 (d, 1H, J = 11 Hz, Ar–H), 7.91 (s, 1H, Ar–H). ^{13}C NMR δ 48.8, 116.8, 118.0, 126.3, 126.7, 127.0, 127.1, 127.5, 128.2, 128.4, 130.4, 131.0, 135.6, 136.3, 138.0, 141.5, 158.5, 160.8, 175.5. MS m/z (%): 473 (2.5, M^+).

5.1.6. Ethyl 2-amino-5-[(3-phenyl or benzyl)-6-substituted-4-oxo-3,4-dihydroquinazolin-2-ylthio]thiazole-4-carboxylate

A mixture of 2-amino-5-bromothiazole-4-carboxylate (**34**, 2.22 g, 0.01 mol), the appropriate 2-thioxo-quinazoline analogs (**18** or **19**, 0.01 mol), anhydrous potassium carbonate (1.5 g, 0.01 mol) in DMF (10 ml) was heated under reflux for 14–16 h. Solvent was then removed under reduced pressure and continued as mentioned under compounds **21**–**24** (Table 1). **39**: ^{1}H NMR (DMSO-d_6) δ 1.54 (t, 3H, J = 14 Hz, CH_2CH_3), 3.15 (s, 6H, OCH_3), 3.52–3.59 (q, 2H, CH_2CH_3), 7.41 (s, 2H, Ar–H), 7.49 (t, 1H, J = 7.5 Hz, Ar–H), 7.52 (t, 2H, J = 7 Hz, Ar–H), 7.84 (d, 2H, J = 8.5 Hz, Ar–H), 12.89 (s, 2H, NH_2). MS m/z (%): 484 (12, M^+). **40**: ^{1}H NMR (DMSO-d_6) δ 1.42 (t, 3H, J = 13.5 Hz, CH_2CH_3), 3.24 (s, 6H, OCH_3), 3.45–3.50 (q, 2H, CH_2CH_3), 5.52 (s, 2H, benzylic–H), 7.41 (t, 3H, J = 8 Hz, Ar–H), 7.50 (s, 2H, Ar–H), 7.67 (d, 2H, J = 7.5 Hz, Ar–H), 11.32 (s, 2H, NH_2). MS m/z (%): 498 (25, M^+).

5.1.7. 2-(3-Phenyl or benzyl-6-substituted-4-oxo-3,4-dihydroquinazolin-2-ylthio)-4-nitrobenzoic acid derivatives (**42**–**45**)

A mixture of 2-chloro-4-nitrobenzoic acid (**41**, 2.01 g, 0.01 mol), the appropriate 2-thioxo-quinazoline analogs (**14**–**17**, 0.01 mol), anhydrous potassium carbonate (1.5 g, 0.01 mol) in DMF (10 ml) was heated under reflux for 24–36 h. Solvent was then removed under reduced pressure and continued as mentioned under compounds **21**–**24** (Table 1). **42**: ^{1}H NMR (DMSO-d_6) δ 2.38 (s, 3H, CH_3), 7.14 (d, 1H, J = 8 Hz, Ar–H), 7.26 (d, 2H, J = 7 Hz, Ar–H), 7.31 (d, 1H, J = 7 Hz, Ar–H), 7.39 (d, 1H, J = 8.5 Hz, Ar–H), 7.42 (t, 1H, J = 7.5 Hz, Ar–H), 7.48 (t, 2H, J = 7 Hz, Ar–H), 7.54 (d, 1H, J = 7 Hz, Ar–H), 7.63 (d, 1H, J = 7.5 Hz, Ar–H), 7.76 (s, 1H, J = 8 Hz, Ar–H), 13.0 (s, 1H, COOH). ^{13}C NMR δ 20.2, 62.9, 115.2, 115.7, 116.0, 126.7, 128.0, 128.7, 128.9, 129.0, 130.2, 131.0, 133.9, 136.6, 137.6, 139.4, 140.6, 159.8, 161.2, 175.5. MS m/z (%): 433 (3.1, M^+). **43**: ^{1}H NMR (DMSO-d_6) δ 2.34 (s, 3H, CH_3), 5.68 (s, 2H, benzylic–H), 7.12 (d, 1H, J = 8 Hz, Ar–H), 7.13 (s, 2H, Ar–H), 7.31–7.34 (m, 4H, Ar–H), 7.35 (d, 1H, J = 8.5 Hz, Ar–H), 7.51 (d, 1H, J = 7 Hz, Ar–H), 7.61 (d, 1H, J = 7 Hz, Ar–H), 7.76 (d, 1H, J = 9.5 Hz,

Ar–H), 13.03 (s, 1H, COOH). ^{13}C NMR δ 20.2, 48.6, 62.9, 113.5, 115.2, 115.7, 126.7, 126.9, 127.1, 127.4, 128.2, 128.3, 131.9, 134.2, 136.2, 136.6, 136.7, 137.1, 137.4, 159.4, 175. MS *m*/*z* (%): 447 (8.5, M^+). **44**: ^{1}H NMR (DMSO-d_6) δ 7.26 (s, 1H, Ar–H), 7.29 (d, 2H, J = 7.5 Hz, Ar–H), 7.34 (d, 2H, J = 7 Hz, Ar–H), 7.43 (d, 2H, J = 8 Hz, Ar–H), 7.48–7.49 (m, 1H, Ar–H), 7.75 (dd, 1H, J = 2.5 Hz, 2 Hz, Ar–H), 7.83 (dd, 1H, J = 2.5 Hz, 2 Hz, Ar–H), 7.88 (t, 1H, J = 4 Hz, Ar–H), 13.16 (s, 1H, COOH). ^{13}C NMR δ 115.8, 117.4, 117.9, 119.0, 126.4, 128.1, 128.7, 128.8, 128.9, 134.9, 135.4, 135.5, 138.4, 138.7, 139.0, 149.9, 158.8, 161.2, 176.1. MS *m*/*z* (%): 454 (7.1, M^+). **45**: ^{1}H NMR (DMSO-d_6) δ 5.56 (s, 2H, benzylic–H), 7.25 (d, 2H, J = 6.5 Hz, Ar–H), 7.29 (t, 2H, J = 7.5 Hz, Ar–H), 7.33 (d, 3H, J = 7 Hz, Ar–H), 7.44 (d, 1H, J = 9 Hz, Ar–H), 7.82 (d, 1H, J = 2 Hz, Ar–H), 7.89 (d, 2H, J = 2 Hz, Ar–H), 13.50 (s, 1H, COOH). ^{13}C NMR δ 115.6, 115.9, 116.2, 116.8, 117.3, 117.8, 118.6, 119.4, 123.6, 124.2, 127.1, 127.2, 128.2, 130.1, 135.9, 143.0, 143.1, 158.6, 176.5, 204.3. MS *m*/*z* (%): 467 (3.3, M^+).

5.1.8. 2-(3-Phenyl or benzyl-6,7-dimethoxy-4-oxo-3,4-dihydroquinazolin-2-ylthio)-4-nitrobenzoic acid derivatives (**46**, **47**)

A mixture of 2-chloro-4-nitrobenzoic acid (**41**, 2.01 g, 0.01 mol), the appropriate 2-thioxo-quinazoline analogs (**18** or **19**, 0.01 mol), anhydrous potassium carbonate (1.5 g, 0.01 mol) in DMF (10 ml) was heated under reflux for 24–36 h. Solvent was then removed under reduced pressure and continued as mentioned under compounds **21**–**24** (Table 1). **46**: ^{1}H NMR (DMSO-d_6) δ 2.89 (s, 6H, OCH_3), 7.31 (d, 2H, J = 7 Hz, Ar–H), 7.42 (t, 1H, J = 7.5 Hz, Ar–H), 7.49 (t, 2H, J = 8 Hz, Ar–H), 7.51 (d, 2H, J = 8 Hz, Ar–H), 7.60 (d, 1H, J = 8.5 Hz, Ar–H), 8.52 (d, 1H, J = 8 Hz, Ar–H), 8.66 (s, 1H, Ar–H), 13.48 (s, 1H, COOH). MS *m*/*z* (%): 479 (5.2, M^+). **47**: ^{1}H NMR (DMSO-d_6) δ 3.87 (s, 6H, OCH_3), 5.53 (s, 2H, benzylic–H), 6.74 (s, 1H, Ar–H), 7.09 (s, 1H, Ar–H), 7.30–7.34 (m, 1H, Ar–H), 7.39 (d, 2H, J = 8 Hz, Ar–H), 7.42 (d, 2H, J = 7.5 Hz, Ar–H), 7.48 (d, 2H, J = 8.5 Hz, Ar–H), 7.56 (s, 1H, Ar–H), 11.36 (s, 1H, COOH). ^{13}C NMR δ 55.7, 56, 97.6, 105.6, 106.1, 107.1, 107.7, 116.5, 116.8, 116.9, 117.8, 118.0, 118.5, 118.9, 119.4, 121.3, 127.9, 128.7, 129.1, 129.4, 129.7, 206.4. MS *m*/*z* (%): 493 (12.1, M^+).

5.2. Dihydrofolate reductase (DHFR) inhibition assay

The assay mixture contained 50 μM Tris–HCl buffer (pH 7.4), 50 μM NADPH, 20 μL DMSO or the same volume of DMSO solution containing the test compounds to a final concentration of 10^{-11}–10^{-5} M, and 0.02 units of bovine liver DHFR, in a final volume of 2.0 ml. After addition of the enzyme, the mixture was incubated at room temperature for 2.0 min, and the reaction was initiated by adding 25 μM FH_2, the change in absorbance (ΔA/min) was measured at 340 nm. The activity under these conditions was linear for 10 min [34] Results are reported as % inhibition of enzymatic activity calculated using the following formula:

$$\%\ \text{Inhibition} = \left(1 - \frac{\Delta A/\text{min}_{\text{test}}}{\Delta A/\text{min}_{\text{DMSO}}}\right) \times 100$$

The % inhibition values were plotted versus drug concentration (log scale). The 50% inhibitory concentration (IC_{50}) of each compound was obtained using the Graph Pad Prism program, version 3 (San Diego, CA).

5.3. Determination of in vitro antimicrobial activity

The primary screen was carried out using the agar disc-diffusion method [35] using Müller-Hinton agar medium. Sterile filter paper discs (8 mm diameter) were moistened with the compound solution in dimethylsulphoxide of specific concentration 200 μg/disc, the antibacterial antibiotic gentamicin, sulphacetamide (100 μg/disc) were carefully placed on the agar cultures plates that had been previously inoculated separately with the microorganisms. The plates were incubated at 37 °C, and the diameter of the growth inhibition zones were measured after 24 h. The minimal inhibitory concentrations (MIC) for the test compounds against the same microorganisms used in the primary screening were carried out using the microdilution susceptibility method in Müller-Hinton Broth [36]. Test compounds, gentamicin, and Sulphacetamide were dissolved in dimethylsulphoxide at concentration of 64 μg/ml. The two fold dilutions of the solution were prepared (64 till 0.5 μg/ml). The microorganism suspensions at 106 CFU/ml concentrations (colony forming unit/ml) were inoculated to the corresponding wells. The plates were incubated at 37 °C for 24 h. The MIC values were determined as the lowest concentration that completely inhibited visible growth of the microorganism as detected by unaided eye.

5.4. Antitumor screening

Under a sterile condition, cell lines were grown in RPMI 1640 media (Gibco, NY, USA) supplemented with 10% fetal bovine serum (Biocell, CA, USA), 5×10^5 cell/ml was used to test the growth inhibition activity of the synthesized compounds. The concentrations of the compounds ranging from 0.01 to 100 mM were prepared in phosphate buffer saline. Each compound was initially solubilized in dimethyl sulfoxide (DMSO), however, each final dilution contained less than 1% DMSO. Solutions of different concentrations (0.2 ml) were pipetted into separate well of a microtiter tray in duplicate. Cell culture (1.8 ml) containing a cell population of 6×10^4 cells/ml was pipetted into each well. Controls, containing only phosphate buffer saline and DMSO at identical dilutions, were also prepared in the same manner. These cultures were incubated in a humidified incubator at 37 °C. The incubator was supplied with 5% CO_2 atmosphere. After 48 h, cells in each well were diluted 10 times with saline and counted by using a coulter counter. The counts were corrected for the dilution [30–33].

5.5. Docking and molecular modeling study

The three-dimensional structures the quinazoline derivatives, which presented best and worst biological profiles, in their neutral forms were constructed using the MOE of Chemical Computing Group Inc software. Lowest energy conformer of each new analog 'global-minima' was docked into the DHFR enzyme-binding domain. For each of the quinazoline analogs, energy minimizations (EM) were performed using 1000 steps of steepest descent, followed by conjugate gradient minimization to a RMS energy gradient of 0.01 kcal/mol Å. The active site of the enzyme was defined using a radius of 10.0 Å around COQ. These selected frames were minimized until RMS deviation values of 0.01 kcal/mol Å were reached for the active-site residues. Energy of binding was calculated as the difference between the energy of the complex and individual energies of the enzyme and ligand [43–46].

5.5.1. Conformational investigation

Initial structures for the investigated molecules were constructed using the HYPERCHEM program version 8.0.5. The MM (calculations *in vacuo*, bond dipole option for electrostatics, PolakeRibiere algorithm, and RMS gradient of 0.01 kcal/mol) conformational searching in torsional space was performed using the 'multiconformer method' [49,50]. Energy minima for investigated compounds were determined by a semi-empirical method AM156 (as implemented in HyperChem 8.0.5). The conformations thus obtained were confirmed as minima by vibrational analysis. Atom-

centered charges for each molecule were computed from the AM1 wave functions (HyperChem 8.0.5) which provides derived charges that closely resemble those obtainable from ab initio 6-31G* calculations [51,52].

5.5.2. Flexible alignment and superposition

The investigated compounds were subjected to flexible alignment experiment using 'Molecular Operating Environment' software (MOE of Chemical Computing Group Inc., on a Core 2 duo 2.3 GHz workstation). The molecules were built using the Builder module of MOE. Their geometry was optimized by using the MMFF94 force field followed by a flexible alignment using systematic conformational search.

Acknowledgments

This research project was supported by a grant from the "Research Center of the Center for Female Scientific and Medical Colleges", Deanship of Scientific Research, King Saud University.

Appendix A. Supplementary data

Supplementary data related to this article can be found at http://dx.doi.org/10.1016/j.ejmech.2012.12.061.

References

[1] H. Masur, Problems in the management of opportunistic infections in patients infected with human immunodeficiency virus, J. Infect. Dis. 161 (1990) 858–864.
[2] E.M. Berman, L.M. Werbel, The renewed potential for folate antagonists in contemporary cancer chemotherapy, J. Med. Chem. 34 (1991) 479–485.
[3] P. Borst, M. Quellette, New mechanism of drug resistance in parasitic protozoa, Annu. Rev. Microbiol. 49 (1995) 427–460.
[4] E. Green, C.H. Demos, in: F.M. Sirotank (Ed.), Folate Antagonists as Therapeutic Agents 2, Academic Press, Orlando, 1984, pp. 191–249.
[5] M.F. Mullarkey, B.A. Blumenstein, W.P. Andrade, G.A. Bailey, I. Olason, C.E. Weizel, Methotrexate in the treatment of corticosteroid-dependent asthma. A double-blind crossover study, N. Engl. J. Med. 318 (1988) 603–607.
[6] E.F. Elslager, J.L. Johnson, L.M. Werbel, Folate antagonists 20. Synthesis, antitumor, and antimalarial properties of trimetrexate and related 6-[(phenylamino)methyl]2,4-quinazolin-diamines, J. Med. Chem. 26 (1983) 1753–1760.
[7] E.M. Grivsky, S. Lee, C.W. Sigel, D.S. Duch, C.A. Nichol, Synthesis and antitumor activity of 2,4-diamino-6(2,5-dimethyloxybenzyl)-5-methylpyrido[2,3-d] pyrimidine, J. Med. Chem. 23 (1980) 327–329.
[8] V. Bavetsias, A.L. Jackman, J.H. Marriott, R. Kimbell, W. Gibson, F.T. Boyle, G.M. Bisset, Folate-based inhibitors of thymidylate synthase, J. Med. Chem. 40 (1997) 1495–1510.
[9] V. Bavetsias, J.H. Marriott, C. Melin, R. Kimbell, Z.S. Matusiak, F.T. Boyle, A.L. Jackman, Design and synthesis of cyclopenta[g]quinazoline-based antifolate as inhibitors of thymidylate synthase and potential antitumor agents, J. Med. Chem. 43 (2000) 1910–1926.
[10] L.M. Werbel, M.J. Degnan, Synthesis and antimalarial and antitumor effects of 2-amino-4-(hydrazino and hydroxyamino)-6-[(aryl)thio]quinazolines, J. Med. Chem. 30 (1987) 2151–2154.
[11] C. Sheng-Li, F. Yu-Ping, J. Yu-Yang, L. Shi-Ying, D. Guo-Yu, L. Run-tao, Synthesis and in vitro antitumor activity of 4(3H)-quinazolione derivatives with dithiocarbamate side chains, Bioorg. Med. Chem. Lett. 15 (2005) 1915–1917.
[12] P.C. Wyss, P. Gerber, P.G. Hartman, C. Hubschwerlen, H. Locher, H. Marty, M. Stahl, Novel dihydrofolate reductase inhibitors. Structure-based versus diversity-based library design and high-throughput synthesis and screening, J. Med. Chem. 46 (2003) 2304–2312.
[13] S.T. Al-Rashood, I.A. Aboldahab, L.A. Abouzeid, A.A.-M. Abdel-Aziz, M.N. Nagi, S.G. Abdul-hamide, K.M. Youssef, A.M. Al-Obaid, H.I. El-Subbagh, Synthesis, dihydrofolate reductase inhibition, and molecular modeling study of some new 4(3H)-quinazolinone analogues, Bioorg. Med. Chem. 14 (2006) 8608–8621.
[14] F.A.M. Al-Omary, L.A. Abou-zeid, M.N. Nagi, E.E. Habib, A.A.-M. Abdel-Aziz, A.S. El-Azab, S.G. Abdel-Hamide, M.A. Al-Omar, A.M. Al-Obaid, H.I. El-Subbagh, Non-classical antifolates. Part 2: synthesis, biological evaluation, and molecular modeling study of some new 2,6-substituted-quinazolin-4-ones, Bioorg. Med. Chem. 18 (2010) 2849–2863.
[15] H.I. El-Subbagh, M.A. El-Sherbeny, M.N. Nasr, F.E. Goda, F.A. Badria, Novel diarylsulphide derivatives as potential cytotoxic agents, Boll. Chim. Farm. 134 (1995) 80–84.
[16] H.I. El-Subbagh, A.H. Abadi, H.A. Al-Khamees, Synthesis and antitumor activity of 9-anilino, phenylhydrazino, and sulphonamido analogues of 2- or 4-methoxy-6-nitroacridines, Arch. Pharm. Pharm. Med. Chem. 330 (1997) 277–282.
[17] A.M. El-Obaid, F.S. El-Shafie, M.S. Al-Mutairi, H.I. El-Subbagh, Synthesis and antitumor activity of certain new substituted 1H-isoindoldione derivatives, Sci. Pharm. 67 (1999) 129–133.
[18] H.I. El-Subbagh, A.H. Abadi, I.E. El-Khawad, K.A. Rashood, Synthesis and antitumor activity of some new substituted quinolin-4-one and 1,7-naphthyridine-4-one analogues, Arch. Pharm. Pharm. Med. Chem. 332 (1999) 19–22.
[19] A.M. Al-Obaid, H.I. El-Subbagh, A.I. Khodair, M.M. El-mazar, 5-Substituted-2-thiohydantoin analogues as a novel class of antitumor agents, Anticancer Drugs 7 (1996) 873–881.
[20] H.I. El-Subbagh, S.M. Abu-Zaid, M.A. Mahran, F.A. Badria, A.M. Al-Obaid, Synthesis and biological evaluation of certain α,β-unsaturated ketones and their corresponding fused pyridines as antiviral and cytotoxic agents, J. Med. Chem. 43 (2000) 2915–2921.
[21] S.H. Al-Madi, A.M. Al-Obaid, H.I. El-Subbagh, The in vitro antitumor assay of 5-(Z)-arylidene-4-imidazolidinone in screens of AIDS-related leukemia and lymphomas, Anticancer Drugs 12 (2001) 835–841.
[22] S.G. Abdel Hamid, H.A. El-Obaid, K.A. Al-Rashood, A.A. Khalil, H.I. El-Subbagh, Substituted quinazolines, 1: synthesis and antitumor activity of certain substituted 2-mercapto-4(3H)-quinazolinone analogues, Sci. Pharm. 69 (2001) 351–366.
[23] A.A. Khalil, S.G. Abdel Hamide, A.M. Al-Obaid, H.I. El-Subbagh, Substituted quinazolines, 2: synthesis and in vitro anticancer evaluation of new 2-substituted mercapto-3H-quinazoline analogues, Arch. Pharm. Pharm. Med. Chem. 336 (2003) 95–103.
[24] H.I. El-Subbagh, A.M. Al-Obaid, 2,4-Disubstituted thiazoles II: a novel class of antitumor agents, synthesis and biological evaluation, Eur. J. Med. Chem. 31 (1996) 1017–1020.
[25] H.I. El-Subbagh, W.A. El-Naggar, F.A. Badria, Synthesis and biological testing of 2,4-disubstituted thiazole derivatives as potential antitumor antibiotics, Med. Chem. Res. 3 (1994) 503–517.
[26] S.G. Abdel Hamid, H.A. El-Obaid, A.A. Al-Majed, H.A. El-Kashef, H.I. El-Subbagh, Synthesis and anticonvulsant activity of some new 4-oxo-3H-quinazoline analogues, Med. Chem. Res. 10 (2001) 378–389.
[27] M.A. Al-Omar, S.G. Abdel Hamide, H.A. Al-Khamees, H.I. El-Subbagh, Synthesis and biological screening of some new substituted-3H-quinazolin-4-one analogues as antimicrobial agents, Saudi Pharm. J. 12 (2004) 63–71.
[28] W.O. Foye, T.L. Lemke, D.A. Williams, Principles of Medicinal Chemistry, fourth ed., Williams and Wilkins, Media, PA, 2005, 442–456.
[29] M.G. Nordberg, K. Kolmodin, J. Aqvist, S.F. Queener, A. Hallberg, Design, synthesis, computational prediction, and biological evaluation of ester soft drugs as inhibitors of dihydrofolate reductase from Pneumocystis carinii, J. Med. Chem. 44 (2001) 2391–2402.
[30] M.R. Grever, S.A. Schepartz, B.A. Chabner, The National Cancer Institute cancer drug discovery and development program, Semin. Oncol. 19 (1992) 622–638.
[31] A. Monks, D. Scudiero, P. Skehan, Feasibility of a high flux anticancer drug screen utilizing a derive panel of human tumor cell lines in culture, J. Natl. Cancer Inst. 83 (1991) 757–766.
[32] M.R. Boyd, K.D. Paull, Some practical considerations and applications of the National Cancer Institute in vitro anticancer drug discovery screen, Drug Rev. Res. 34 (1995) 91–109.
[33] P. Skehan, R. Storeng, D. Scudiero, A. Monks, J. McMahon, D. Vistica, J.R. Warren, H. Bokesch, S. Kenney, M.R. Boyd, New colorimetric cytotoxicity assay for anticancer-drug screening, J. Natl. Cancer Inst. 82 (1990) 1107–1112.
[34] R. Pignatello, G. Sapmpinato, V. Sorrenti, L. Vicari, C. Di-Giacomo, A. Vanella, G. Puglisi, Aliphatic α-γ-bis (amides) of methotrexate. Influence of chain length on in vitro activity against sensitive and resistant tumor cells, Pharm. Pharmacol. Commun. 5 (1999) 299–504.
[35] National Committee for Clinical Laboratory Standards (NCCLS), Approved Standard Document M-7A (1985). Villanova, PA.
[36] P.R. Murray, E.J. Baron, M.A. Pfaller, F.C. Tenover, R.H. Yolken, in: G.L. Wood, J.A. Washington (Eds.), Manual of Clinical Microbiology, American Society for Microbiology, Washington D.C., 1995.
[37] A. Gangjee, H.D. Jain, Antifolates – past, present and future, Curr. Med. Chem. Anticancer Agents 4 (2004) 405–410.
[38] D.C.M. Chan, A.C. Anderson, Towards species-specific antifolates, Curr. Med. Chem. 13 (2006) 377–398.
[39] J.R. Schnell, H.J. Dyson, P.E. Wright, Structure, dynamics, and catalytic function of dihydrofolate reductase, Annu. Rev. Biomol. Struct. 33 (2004) 119–140.
[40] J. Feeney, NMR studies of ligand binding to dihydrofolate reductase, Angew. Chem. Int. Ed. 39 (2000) 290–312.
[41] J.M. Blaney, C. Hansch, C. Silipo, A. Vittoria, Structure-activity relationships of dihydrofolate reductase inhibitors, Chem. Rev. 84 (1984) 333–407.
[42] V. Cody, S.F. Zakrzewski, Molecular structures of 2,4-diaminopyrimidine antifolates with antineoplastic activity, J. Med. Chem. 25 (1982) 427–430.
[43] M.L. López-Rodríguez, M. Murcia, B. Benhamú, A. Viso, M. Campillo, L. Pardo, 3-D-QSAR/CoMFA and recognition models of benzimidazole derivatives at the 5-HT(4) receptor, Bioorg. Med. Chem. Lett. 11 (2001) 2807–2811.
[44] PowerFit, Microsimulation (1996). Mahwah, NJ, USA.
[45] V.M. Gokhale, V.M.J. Kulkarni, Selectivity analysis of 5-(arylthio)-2,4-diaminoquinazolines as inhibitors of Candida albicans dihydrofolate reductase by molecular dynamics simulations, J. Comput. Aided Mol. Des. 14 (2000) 495–506.

[46] E. Klon, A. Heroux, L.J. Ross, V. Pathak, C.A. Johnson, J.R. Piper, D.W. Borhani, Atomic structures of human dihydrofolate reductase complexed with NADPH and two lipophilic antifolates at 1.09 a and 1.05 a resolution, J. Mol. Biol. 320 (2002) 677–693.
[47] C.-M. Chu, S. Gao, M.N.V. Sastry, C.-F. Yao, Iodine-catalyzed Michael addition of mercaptans to α,β-unsaturated ketones under solvent-free conditions, Tetrahedron Lett. 46 (2005) 4971–4974.
[48] V. Cody, C.H. Schwalbe, Structural characteristics of antifolate dihydrofolate reductase enzyme interactions, Crystallogr. Rev. 12 (2006) 301–333.
[49] S. Profeta, N.L. Allinger, Molecular mechanics calculations on aliphatic amines, J. Am. Chem. Soc. 107 (1985) 1907–1918.
[50] N.L. Allinger, Conformational analysis. 130. MM2. A hydrocarbon force field utilizing V_1 and V_2 torsional terms, J. Am. Chem. Soc. 99 (1977) 8127–8134.
[51] P. Labute, C. Williams, M. Feher, E. Sourial, J.M. Schmidt, Flexible alignment of small molecules, J. Med. Chem. 44 (2001) 1483–1490.
[52] S. Kearsley, G.M. Smith, An alternative method for the alignment of molecular structures: maximizing electrostatic and steric overlap, Tetrahedron Comput. Methodol. 3 (1990) 615–633.